Am J Cancer Res 2025;15(5):2140-2152
www.ajcr.us /ISSN:2156-6976/ajcr0164549

Original Article

Cynaropicrin induces the apoptosis of colorectal cancer cells by elevating reactive oxygen species and activating the JNK/p38 MAPK

Si Yeong Seo[1*], Sang Hoon Joo[2*], Seung-On Lee[1], Ki-Taek Kim[1,3], Yung Hyun Choi[4], Goo Yoon[3], Jin Woo Park[1,3], Jung-Hyun Shim[1,3,5]

[1]Department of Biomedicine, Health and Life Convergence Sciences, BK21 Four, College of Pharmacy, Mokpo National University, Muan 58554, Republic of Korea; [2]College of Pharmacy, Daegu Catholic University, Gyeongsan 38430, Republic of Korea; [3]Department of Pharmacy, College of Pharmacy, Mokpo National University, Muan 58554, Republic of Korea; [4]Department of Biochemistry, College of Korean Medicine, Dong-Eui University, Busan 47227, Republic of Korea; [5]The China-US (Henan) Hormel Cancer Institute, Zhengzhou 450008, Henan, P. R. China. [*]Equal contributors.

Received March 14, 2025; Accepted April 21, 2025; Epub May 15, 2025; Published May 30, 2025

Abstract: The development of new therapeutics for colorectal cancer (CRC) is urgently needed to address the limitations of current treatments. This study was performed to investigate the anticancer activity of cynaropicrin (a natural product) in CRC HCT116 cells and an oxaliplatin (Ox)-resistant HCT116 strain (HCT116-OxR). MTT cell viability assays showed that cynaropicrin inhibited the growth of HCT116 and HCT116-OxR cells in a dose- and time-dependent manner. Cynaropicrin also induced apoptosis, as identified by an Annexin V-FITC/PI double staining, and this apoptosis was accompanied by the phosphorylations of JNK and p38 MAPK. In addition, treatment with the kinase-specific inhibitors SP600125 and SB203580 confirmed that this apoptosis was mediated by JNK and p38 MAPK. Flow cytometry analysis using the CellROX™ kit showed cynaropicrin increased reactive oxygen species (ROS) levels, and N-acetylcysteine pretreatment confirmed ROS mediated the cytotoxicity of cynaropicrin. Flow cytometry with propidium iodide staining and western blot analysis indicated that cynaropicrin induced cell cycle arrest at the G2/M phase by modulating cell cycle regulators, and western blot analysis revealed that cynaropicrin altered the balance of Bcl-2 family proteins. Also, flow cytometry using the Muse™ Multi-Caspase Kit showed cynaropicrin activated multiple caspases, the crucial roles of which were confirmed using the pan-caspase inhibitor Z-VAD-FMK. In conclusion, cynaropicrin demonstrated anticancer activity against CRC cells by elevating ROS levels, activating JNK and p38 MAPK, and inducing cell cycle arrest leading to apoptosis. Further studies are warranted to evaluate the therapeutic potential of cynaropicrin in CRC.

Keywords: Cynaropicrin, colorectal cancer, reactive oxygen species, JNK, p38

Introduction

Cancer remains one of the leading causes of death worldwide. More than two million Americans are diagnosed with cancer each year, and more than half a million succumb to the disease [1]. Colorectal cancer (CRC) is the third most common cancer type and claims many lives annually [2]. Encouragingly, the past decade has witnessed a slight decline in the incidence of CRC, which has been attributed to regular screenings, reduced smoking rates, and other factors. However, it is concerning that the incidence of CRC is increasing among those aged less than 50. In this population, the number of CRC patients is rising by 1-2% each year, and this trend is threatening to reverse overall progress in cancer prevention and to increase the burden on healthcare systems [3]. Chemotherapy can be administered to CRC patients after surgery or used to treat metastatic disease [4]. Oxaliplatin (Ox) is the chemotherapeutic agent of choice for treating CRC, but drug resistance and other complications limit its use [5]. Many attempts have been made to develop more effective chemotherapeutic agents to overcome the limitations of current treatments, which include drug resistance and

https://doi.org/10.62347/OPNG2835

low bioavailability [6]. Natural products represent a valuable repertoire of anticancer drugs and drug candidates [7], and numerous compounds, such as podophyllotoxin [8], taxol [9], and vinblastine [10], have been reported to exhibit anticancer activity. Various mechanisms contribute to the anticancer activity of natural products, such as apoptosis [11], the inhibition of angiogenesis [12], the modulation of immune response [13], and the regulation of reactive oxygen species (ROS) [14].

ROS play a crucial role in the regulation of cancer cell survival and death. Although short-lived, ROS are highly reactive and significantly affect cancer cells [15]. At low levels, ROS promote cancer cell growth [16], but at elevated levels, ROS cause cell death via mitochondrial disruption [17], death receptors [18], and the perturbation of endoplasmic reticulum (ER) [19]. Furthermore, cancer cell apoptosis may be induced at high ROS levels [20].

Cynaropicrin is a sesquiterpene lactone initially isolated from the artichoke (*Cynara scolymus L)* [21] and has been reported to possess multiple biological activities, including the specific apoptosis of melanoma cells [22]. Although little is known about the anticancer activity of cynaropicrin in CRC cells, it has been reported to modulate ROS in various leukocyte, thyroid, and melanocyte cancer cells [22-24]. In this study, we investigated the anticancer activity of cynaropicrin in Ox-sensitive and -resistant CRC cells, that is, HCT116 and HCT116-OxR cells, respectively, which allowed us to explore Ox resistance [25]. Our results indicate that cynaropicrin has potential therapeutic use for treating Ox-resistant CRC.

Material and methods

Reagent and antibodies

Cynaropicrin (MW 346.4, 98% purity) was obtained from Cayman Chemical (Ann Arbor, MI, USA). Cell culture media (MEM and RPMI-1640) were from WELGENE (Gyeongsan, Gyeongsangbuk-do, Republic of Korea). Fetal bovine serum (FBS), phosphate buffered saline (PBS), penicillin/streptomycin (p/s), and trypsin were purchased from Gibco (Carlsbad, CA, USA). Basal Medium Eagle (BME) and N-acetylcysteine (NAC) were obtained from Sigma-Aldrich (St. Louis, MO, USA). 3-(4,5-dimethyl-2-thiazolyl)-2,5-diphenyl-2-H-tetrazolium bromide (MTT) was from Biosesang (Yongin, Gyeonggi-do, Republic of Korea). Primary antibodies against apoptotic protease activating factor-1 (Apaf-1) (sc-33870), Bax (sc-20067), Bcl-xL (sc-8392), Bcl-2 (sc-7382), Bid (sc-56025), caspase-3 (sc-7148), cdc2 (sc-8395), cyclin B1 (sc-7393), p21 (sc-6246), p27 (sc-56338), and β-actin (sc-47778) were obtained from Santa Cruz Biotechnology (Dallas, TX, USA). Antibodies against phospho (p)-JNK (Thr183/Tyr185) (#9251), JNK (#9252), p-p38 (Thr180/Tyr182) (#9211), and p38 (#9212) were purchased from Cell Signaling Biotechnology (Beverly, MA, USA).

Cell culture and treatment

HCT116 and HEKa cells were obtained from ATCC (Manassas, VA, USA). HCT116 and HEKa cells were maintained in RPMI-1640 and DMEM medium supplemented with 10% FBS and 1% p/s, respectively. The oxaliplatin-resistant HCT-116 cell line (HCT116-OxR) were acquired from MD Anderson. HCT116-OxR cells were grown in MEM medium supplemented with 10% FBS and 1% p/s. To promote optimal growth, the culture medium was enriched with 1% sodium pyruvate, 1% MEM nonessential amino acids, and 1% MEM vitamins. We treated the cells with 2 μM Ox. To achieve a specific result, the cells were treated with cynaropicrin (0, 0.1, 0.2, and 0.4 μg/mL) for 24 or 48 h. The HCT116 and HCT116-OxR cells were pretreated with SP600125 (JNK inhibitor, 4 μM), SB203580 (p38 MAPK inhibitor, 5 μM), NAC (ROS inhibitor, 4 mM) or Z-VAD-FMK (pan-caspase inhibitor, 4 μM) for 3 h and exposed to cynaropicrin (0.4 μg/mL) for 48 h.

Cell viability assay

HCT116 cells (5×10^3 cells/well), HCT116-OxR cells (4×10^3 cells/well), or HEKa cells (8×10^3 cells/well) were cultured in a 96-well plate for 24 hours with 5% CO_2 at 37°C. The cells were then treated with either cynaropicrin (0, 0.1, 0.2, and 0.4 μg/mL) or Ox (2 μM) for 24 and 48 h. After a 1 hour incubation period, 30 μl of MTT reagent was added to each well. The media was removed, and the formed insoluble formazan crystals were dissolved in DMSO and quantified at 570 nm using a microplate reader (Thermo Fisher Scientific, Waltham, USA). Data from four replicate experiments were used to determine the relative cell viability.

Anchorage-independent soft agar assay

HCT116 and HCT116-OxR cells were seeded at a density of 8 × 10^3 cells/well in 6-well plates and treated with medium containing 0.3% agar and the indicated concentrations of cynaropicrin and Ox. After 10 days of culture, the cells were photographed under an optical microscope (Leica Microsystems, Wetzlar, Germany) and the number and size of colonies were counted using i-Solution™ (Vancouver, BC, Canada).

Western blotting

Cells were lysed using PRO-PREP™ protein extraction solution, and protein concentrations were measured using a BCA assay kit (Bio-Rad, CA, USA). Equal amounts of protein were separated by SDS-PAGE and transferred to PVDF membranes. After blocking and incubation with primary and secondary antibodies, immunoreactive bands were visualized using chemiluminescence and detected with an ImageQuant™ LAS500 System (GE Healthcare, Uppsala, Sweden) and an iBright™ CL1500 Imaging System (Thermo Fisher Scientific). Blot images were quantified using ImageJ software (NIH, Bethesda, MD, USA) and relative band intensities were normalized to loading controls.

Cell cycle analysis

HCT116 and HCT116-OxR cells were treated with various concentrations of cynaropicrin. Cells were then fixed in 70% ethanol and kept at -20°C for at least 24 h. Ethanol was removed and treated with RNase A (2.5 µL) for 15 min at RT. Propidium iodide (PI) Reagent (5 µL) was then added and analyzed on a MACSQuant® Analyzer 16 flow cytometer (Miltenyi Biotec, Bergisch Gladbach, Germany).

Analysis of Reactive Oxygen Species (ROS)

HCT116 and HCT116-OxR cells were incubated with CellROX™ Green Reagent for 30 minutes at 37°C. Intracellular ROS levels were subsequently quantified using a MACSQuant® Analyzer 16 Flow Cytometer.

Annexin V-FITC/PI double staining assay

HCT116 and HCT116-OxR cells were treated with cynaropicrin for 48 hours. Following treatment, cells were harvested, stained with Annexin V-FITC (Miltenyi Biotec), and incubated for 15 minutes at room temperature. Subsequently, PI was added to the cell suspension. The stained cells were then analyzed using a MACSQuant® Analyzer 16 Flow Cytometer to determine the percentage of cells in early and late apoptotic stages.

Multi-caspase assay

To assess the activation of multiple caspases (caspase-1, -3, -4, -5, -6, -7, -8, and, -9), CRC cells were exposed to various concentrations of cynaropicrin. The Muse™ Multi-Caspase Kit (MCH100109) was employed to detect activated caspases in treated cells. Cells were incubated with the kit's reagent for 30 minutes at 37°C, followed by a 5-minute incubation with 7-AAD working solution at room temperature. Activated caspase cells were subsequently analyzed using the Muse™ Cell Analyzer.

Statistical analysis

Data are presented as the mean ± SD. Statistical significance was determined by one-way or two-way ANOVA followed by Tukey's multiple comparison test using KaleidaGraph 4.5 software (Synergy Software, MT Penn, PA, USA). Statistical significance was set at $*P < 0.05$, $**P < 0.01$, and $***P < 0.001$.

Results

Cynaropicrin inhibited the growth of CRC cells

To evaluate the cytotoxicity of cynaropicrin, CRC HCT116, and HCT116-OxR cells were treated with cynaropicrin for 24 or 48 h, and cell viability was determined using an MTT assay. The viabilities of HCT116 cells treated with cynaropicrin at 0.1, 0.2, or 0.4 µg/mL for 48 h were 67.32%, 58.46%, and 45.29%, respectively, compared to the vehicle control. In HCT116-OxR cells, corresponding values were 76.49%, 46.94%, and 38.38%, respectively. The cell viability of HCT116 cells treated with Ox was 37.54%, whereas the corresponding value for HCT116-OxR was 93.88%, confirming the higher sensitivity of HCT116 cells to Ox. Cell viability assays showed cynaropicrin inhibits the growth of CRC cells in a time- and concentration-dependent manner. After incu-

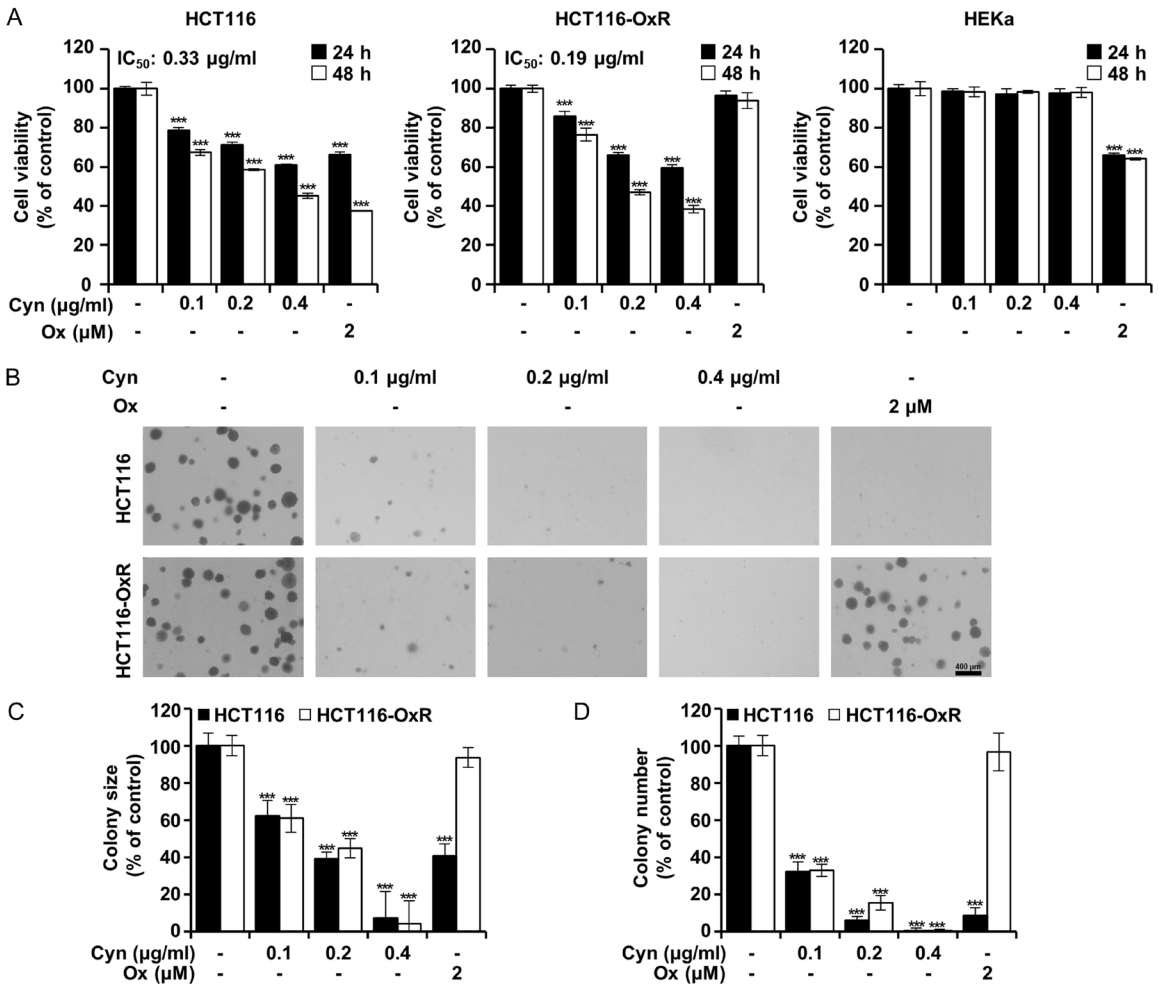

Figure 1. Inhibition of CRC cell growth by cynaropicrin. A. HCT116, HCT116-OxR, and HEKa cells were treated with various concentrations (0, 0.1, 0.2, or 0.4 μg/mL) of cynaropicrin or oxaliplatin (Ox, 2 μM) for 24 or 48 h. Cell viabilities were determined using an MTT assay. B-D. Anchorage-independent colony growth was assessed using a soft agar assay (incubation for 10 days). B. Micrograph of CRC cells at day 10 after treatment. C, D. Sizes and numbers of colonies. The data are presented as the mean ± SD, n = 4. ***P < 0.001 versus non-treated controls.

bation for 48 h, the IC_{50} values of cynaropicrin for HCT116 and HCT116-OxR cells were 0.33 and 0.19 μg/mL, respectively. For comparison purposes, we evaluated the cell viability of human skin keratinocyte HEKa cells, which are noncancerous. The viabilities of HEKa cells treated with cynaropicrin at 0.1, 0.2, or 0.4 μg/mL were 98.22%, 98.25%, and 98.01%, respectively, versus the vehicle control. In contrast, cell viability was only 64.17% when HEKa cells were treated with Ox (**Figure 1A**). In addition, a soft agar colony formation assay (**Figure 1B**) confirmed the selective cytotoxicity of cynaropicrin in HCT116 cells: the size and number of colonies decreased significantly as cynaropicrin concentration increased (**Figure 1C**, **1D**).

Cynaropicrin induced the apoptosis of CRC cells by activating JNK/p38 MAPK signaling

We then examined the apoptotic effect of cynaropicrin in HCT116 and HCT116-OxR cells. CRC cells were treated with cynaropicrin at 0.1, 0.2, or 0.4 μg/mL for 48 h, and then subjected to flow cytometry analysis with Annexin V-FITC/PI double staining. Compared to vehicle controls, we observed an increase in the proportion of cells in the early apoptotic phase (Annexin V-FITC+ and PI-). In HCT116 cells, cynaropicrin treatment at 0.1, 0.2, or 0.4 μg/mL increased the proportion of cells in the early apoptotic phase from 1.00% to 2.10%, 4.36%, and 8.68%, respectively. The corresponding

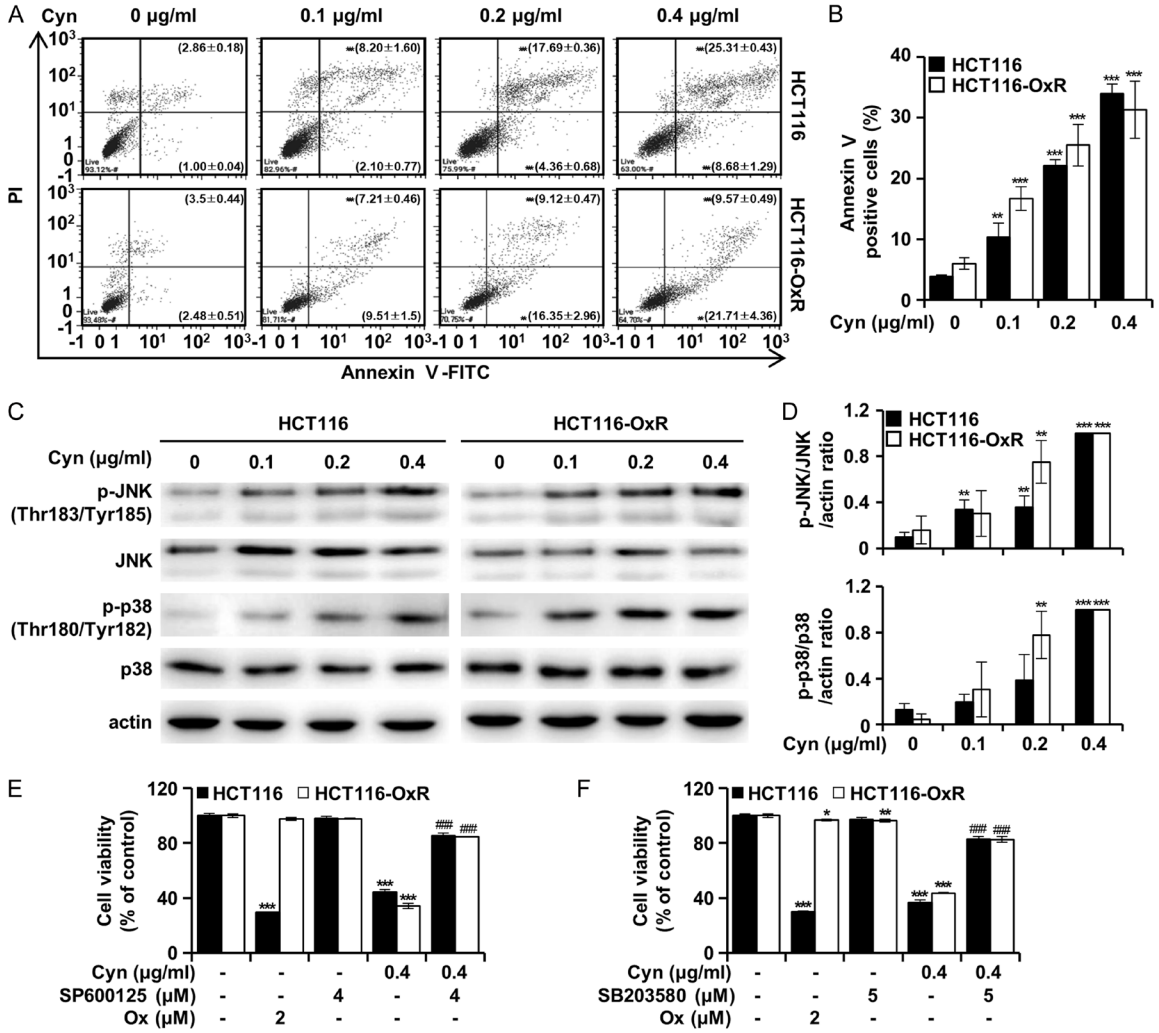

Figure 2. Induction of apoptosis by JNK/p38 MAPK signaling in CRC cells. A-D. CRC cells were treated with cynaropicrin (0, 0.1, 0.2, or 0.4 μg/mL) for 48 h. A. Flow cytometry analysis with Annexin V-FITC/PI double staining. B. Histogram showing the proportion of cells undergoing apoptosis. C. Western blot analysis of p-JNK, JNK, p-p38, and p38 protein levels. Actin was used as a loading control. D. Histogram depicting the p-JNK/JNK and p-p38/p38 ratios. E, F. CRC cells were pretreated with SP600125 (4 μM) or SB203580 (5 μM) for 3 h before cynaropicrin treatment. Cell viabilities were determined using an MTT assay. Means ± SDs of four independent experiments. *P < 0.05, **P < 0.01, and ***P < 0.001 versus non-treated controls. ###P < 0.001 versus cynaropicrin-treated cells.

values for HCT116-OxR cells increased from 2.48% to 9.51%, 16.35%, and 21.71%. Moreover, the population of cells in late apoptosis phase (Annexin V-FITC+ and PI+) increased from 2.86% to 8.20%, 17.69%, and 25.31% for HCT116 cells, and from 3.5% to 7.21%, 9.12%, and 9.57% for HCT116-OxR cells (**Figure 2A**, **2B**). These results indicate that cynaropicrin induced early and late apoptosis in CRC cells.

Western blot analysis was performed to examine the effect of cynaropicrin on the MAPK signaling pathway. The results showed that cynaropicrin treatment increased levels of the phosphorylated forms of JNK and p38 MAPK (**Figure 2C**, **2D**). To determine whether the activations of JNK and p38 are prerequisites for cynaropicrin-induced apoptosis, CRC cells were pretreated with pharmacological inhibitors of JNK and p38 MAPK. Specifically, SP600125 (a JNK inhibitor, 4 μM) or SB203580 (a p38 inhibitor, 5 μM) was administered prior to cynaropicrin treatment (0.4 μg/mL for 48 h), and cell viabilities were assessed. The results showed that these inhibitors almost completely blocked cynaropicrin-induced cytotoxicity (**Figure 2E**, **2F**).

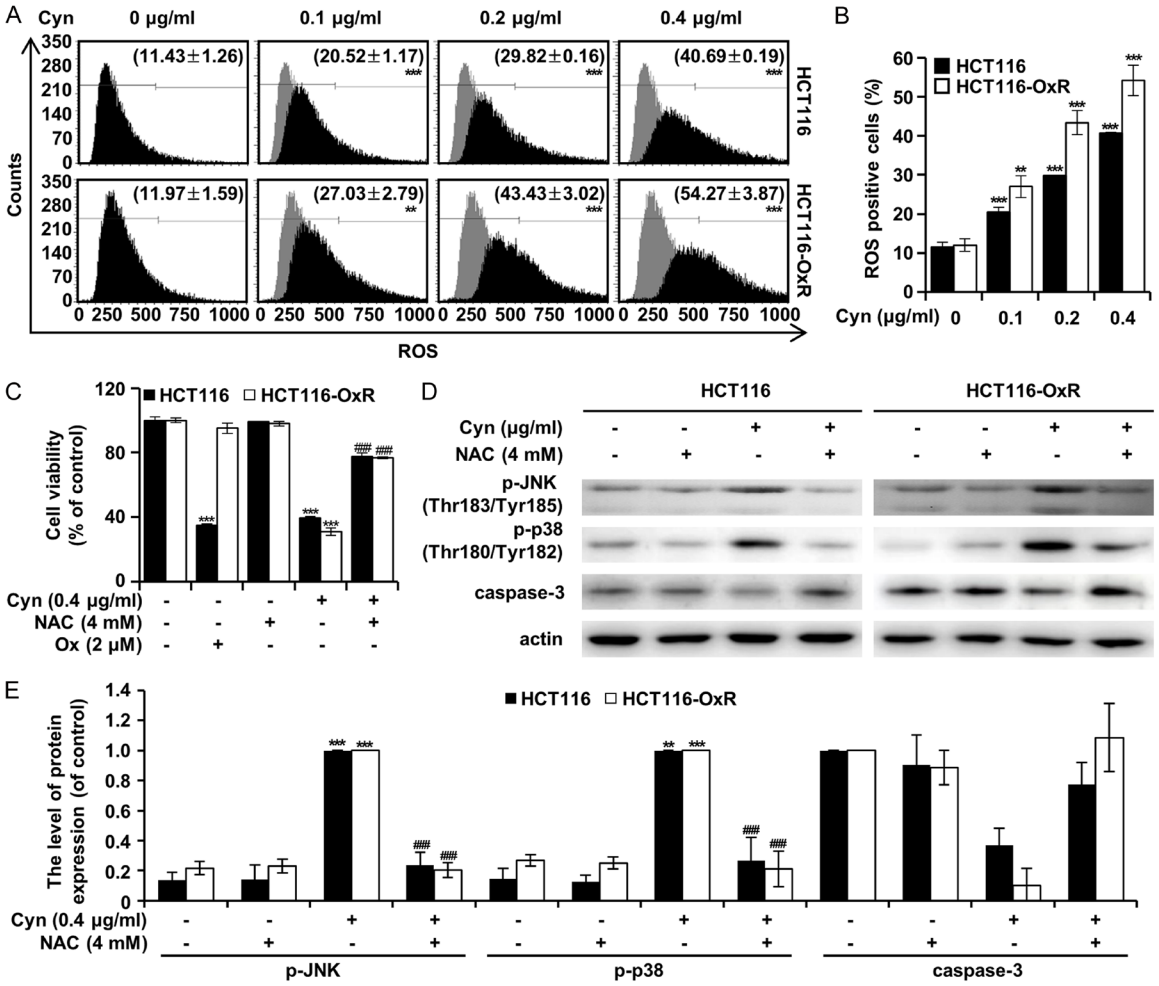

Figure 3. Generation of ROS in CRC cells. CRC cells were treated with cynaropicrin at 0, 0.1, 0.2, or 0.4 μg/mL for 48 h. (A) Flow cytometry analysis using the CellROX™ kit. (B) Proportion of ROS-positive cells in (A). (C-E) CRC cells were pretreated with N-acetylcysteine (NAC, 4 mM) for 3 h and then treated with cynaropicrin for 48 h. (C) Cell viabilities as determined by the MTT assay. (D) Western blot analysis of p-JNK, p-p38, caspase-3. Actin was used as the loading control. (E) Relative level of p-JNK, p-p38, and caspase-3 normalized versus actin. Data are the means of quadruplicate wells. $^{**}P < 0.01$ and $^{***}P < 0.001$ versus non-treated controls. $^{###}P < 0.001$ versus cynaropicrin-treatment.

Cynaropicrin induced the generation of ROS in CRC cells

HCT116 and HCT116-OxR cells treated with cynaropicrin for 48 h (0.1, 0.2, or 0.4 μg/mL) were subjected to flow cytometry analysis with CellROX™ Green Reagent staining, and ROS levels were then determined to investigate the effect of cynaropicrin on ROS generation in CRC cells. Cynaropicrin treatment at 0.1, 0.2, or 0.4 μg/mL increased the percentage of HCT116 cells with excessive ROS levels from 11.43% to 20.52%, 29.82%, and 40.69%, respectively. The corresponding value for HCT116-OxR cells increased from 11.97% to 27.03%, 43.43%, and 54.27% (**Figure 3A**, **3B**). To determine whether the generation of excessive ROS is an essential requirement for cynaropicrin-induced cytotoxicity, CRC cells were pretreated with the ROS scavenger NAC at 4 mM. The MTT cell viability assay revealed that NAC pretreatment significantly prevented cynaropicrin-induced cytotoxicity. In HCT116 cells, viability decreased to 39.45% by cynaropicrin treatment but was 77.36% after NAC pretreatment. Similarly, in HCT116-OxR cells, cynaropicrin reduced viability to 31.21%, but NAC pretreatment increased viability to 76.92% (**Figure 3C**). Furthermore, western blot revealed that ROS generation in cynaropicrin-treated cells coincided with an increase in the levels of phosphorylated JNK and p38 MAPK (**Figure 3D**, **3E**).

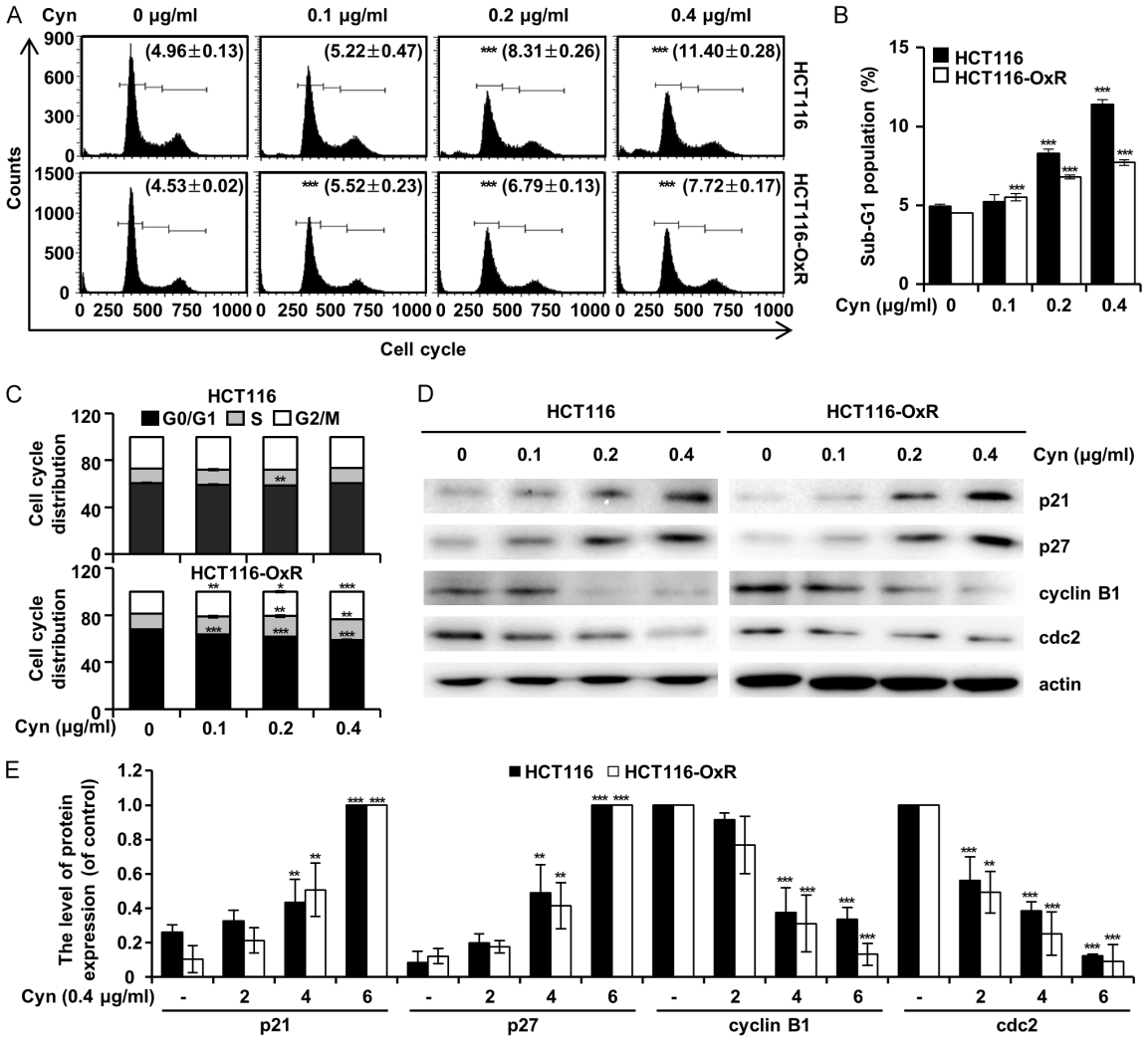

Figure 4. Cell cycle arrest in cynaropicrin-induced CRC cells. (A-C) CRC cells were treated with cynaropicrin at 0, 0.1, 0.2, or 0.4 μg/mL for 48 h. (A) Histogram of flow cytometry results with propidium iodide staining. (B) The proportion of the sub-G1 population in (A). (C) Cell cycle distribution of G0/G1, S, and G2/M phase populations. *P < 0.05, **P < 0.01, and ***P < 0.001 versus untreated controls. (D) Western blot analysis of p21, p27, cyclin B1, and cdc2. Actin was used as a loading control. (E) Relative ratios of p21, p27, cyclin B1, and cdc2 normalized versus actin. Results are as mean ± SD of four quadruplicate experiments. *P < 0.05, **P < 0.01, and ***P < 0.001 compared to untreated controls.

Cynaropicrin inhibited the growth of CRC cells by modulating the cell cycle at the G2/M phase

To determine the effect of cynaropicrin on the cell cycle, HCT116 and HCT116-OxR cells treated with cynaropicrin at 0.1, 0.2, or 0.4 μg/mL for 48 h were analyzed by flow cytometry with PI staining (**Figure 4A**). Noticeably, cynaropicrin treatment increased the proportion of HCT116 and HCT116-OxR cells in the sub-G1 phase. In HCT116 cells, the proportion of cells in the sub-G1 phase increased from 4.96% to 5.22%, 8.31%, and 11.40% by cynaropicrin at 0.1, 0.2, or 0.4 μg/mL. Similarly, for HCT116-OxR cells, the value increased from 4.53% to 5.52%, 6.79%, and 7.72%, respectively, suggesting cynaropicrin promoted apoptosis (**Figure 4B**). The cell cycle distribution (**Figure 4C**) showed that cynaropicrin increased the proportion of cells in the G2/M phase. This was more apparent for HCT116-OxR cells, which also showed a concurrent reduction in the S phase. In addition, western blot indicated that p21 and p27 (both cyclin-dependent kinase inhibitors) were upregulated by increasing cynaropicrin concen-

tration (**Figure 4D**, **4E**). On the other hand, levels of cyclin B1 and cdc2 (key regulators of G2/M transition [26]) were downregulated by cynaropicrin. These effects were observed in HCT116 and HCT116-OxR cells, but HCT116-OxR cells proved to be more sensitive to cynaropicrin.

Cynaropicrin induced the apoptosis of CRC cells by altering the balance in Bcl-2 family proteins and activating caspases

We also examined whether cynaropicrin modulated the balance in Bcl-2 family proteins, which can lead to the intrinsic mitochondrial apoptosis. Western blot revealed a decrease in the protein levels of Bcl-2, Bcl-xL, and Bid and of full-length caspase-3 in CRC cells treated with cynaropicrin. On the other hand, Bax and Apaf-1 levels were increased by cynaropicrin (**Figure 5A**). To examine the activities of multiple caspases, HCT116 and HCT116-OxR cells treated with cynaropicrin at 0.1, 0.2, or 0.4 μg/mL for 48 h were subjected to flow cytometry using the Muse™ Multi-caspase kit. For flow cytometry quadrant analysis, cells were categorized as: live caspase-positive, live caspase-negative, dead caspase-positive, and dead caspase-negative (**Figure 5B**). For HCT116 cells, cynaropicrin treatment at 0.1, 0.2, or 0.4 μg/mL increased the proportion of live or dead caspase-positive cells from 3.40% to 26.92%, 32.97%, and 44.78%. The corresponding values for HCT116-OxR cells increased from 4.42% to 19.20%, 25.97%, and 39.83% (**Figure 5C**). To determine whether caspase activations mediated cynaropicrin-induced apoptosis, HCT-116 and HCT116-OxR cells were pretreated with Z-VAD-FMK 4 μM for 3 h. When HCT116 and HCT116-OxR cells were treated with cynaropicrin, cell viabilities dropped to 34.02% and 43.18%, respectively, but when pretreated with Z-VAD-FMK cell viabilities dropped to 93.64% and 94.83%, respectively (**Figure 5D**).

Discussion

This study was undertaken to determine whether cynaropicrin inhibits the growth of oxaliplatin (Ox)-sensitive HCT116 and Ox-resistant HCT-116-OxR cells. Our results show that cynaropicrin induces apoptosis in these cells by elevating ROS levels and activating the JNK/p38 MAPK signaling pathway.

Ox is a third-generation platinum-based anticancer agent and a key component in colorectal cancer (CRC) treatments [27]. However, its side effects and vulnerability to resistance development necessitate the development of more effective chemotherapeutics. In the present study, cynaropicrin effectively inhibited the growth of HCT116 CRC cells regardless of Ox-resistance (**Figure 1**), and cynaropicrin significantly and dose-dependently reduced cancer cell viability. Furthermore, cynaropicrin exhibited negligible cytotoxicity in HEKa cells, suggesting that the cytotoxic effect of cynaropicrin is limited to cancer cells.

The induction of cancer cell apoptosis is an excellent therapeutic strategy because it results in the specific removal of cancer cells without damaging other tissues, and in the present study, the Annexin V-FITC/PI double staining assay showed that cynaropicrin did indeed induce the apoptosis of CRC cells (**Figure 2A**, **2B**). JNK and p38 MAPK signaling has been well documented to regulate the progress of apoptosis [28, 29], and we observed cynaropicrin concentration-dependently increased levels of phosphorylated JNK and p38 (**Figure 2C**, **2D**). In addition, the kinase-selective inhibitors SP600125 (a JNK inhibitor) and SB203580 (a p38 inhibitor) prevented cynaropicrin-induced CRC apoptosis, supporting the notion that JNK and p38 mediate cynaropicrin-induced apoptosis in CRC cells (**Figure 2E**, **2F**).

Cancer proliferation is usually accompanied by elevated ROS levels in multiple cancers, including esophageal cancer, lung cancer, and CRC [16, 30, 31]. These increases in ROS levels in cancer tissues could benefit cancer cell growth by sustaining growth signaling [32]. However, greater ROS increases can lead to oxidative stress and cancer cell apoptosis [33, 34]. Our experimental data showed that cynaropicrin increased ROS levels in Ox-sensitive and Ox-resistant HCT116 cells (**Figure 3A**, **3B**). In addition, NAC pretreatment confirmed the generation of excessive ROS mediated cynaropicrin-induced apoptosis (**Figure 3C**). Furthermore, NAC pretreatment prevented not only prevented cynaropicrin-induced cytotoxicity but also prevented the phosphorylations of JNK and p38 MAPK, suggesting that the generation of excessive ROS preceded the phosphorylation (**Figure 3D**, **3E**). Thus, it appears ROS genera-

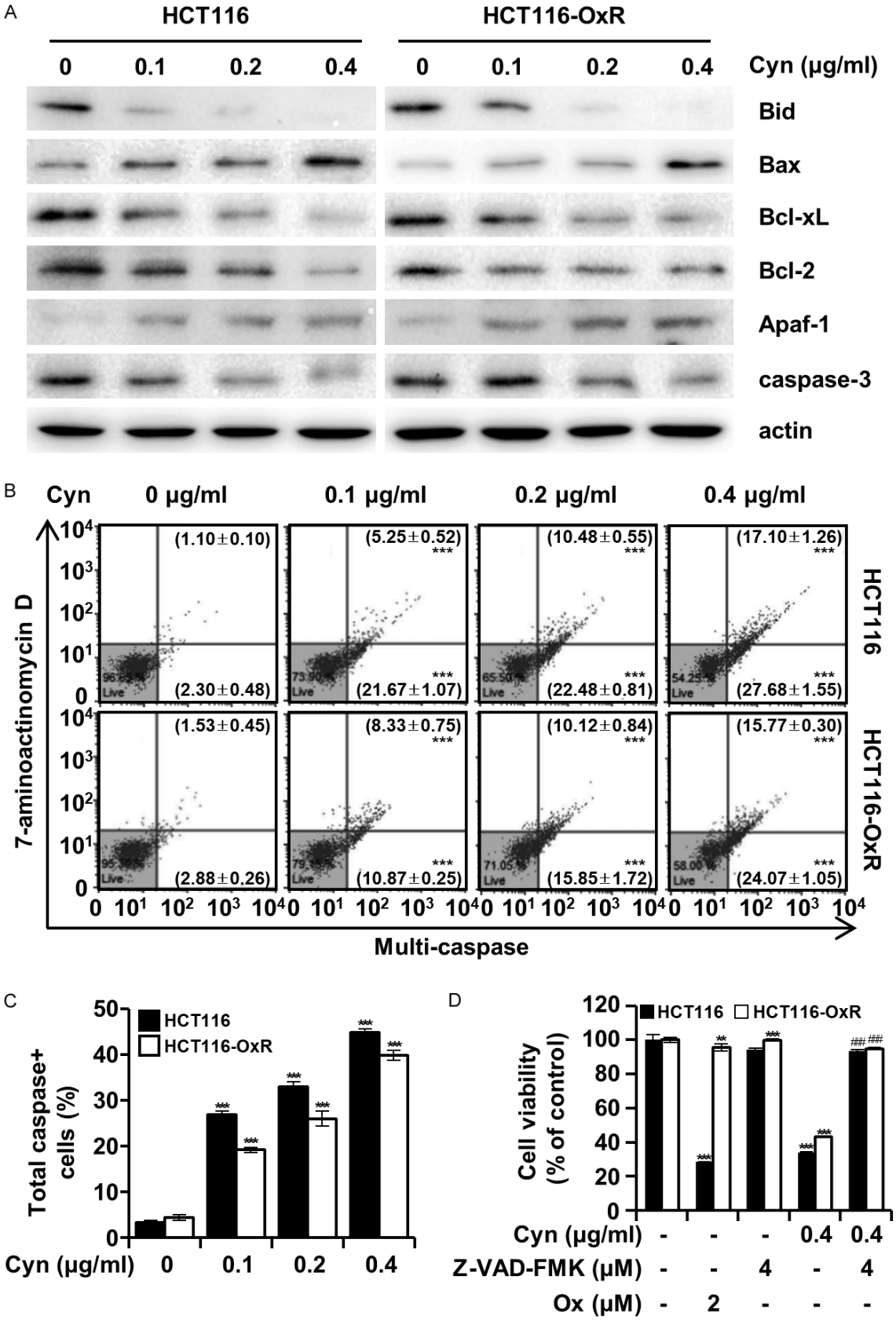
A
HCT116
HCT116-OxR
0
0.1
0.2
0.4
0
0.1
0.2
0.4
Cyn (μg/ml)
Bid
Bax
Bcl-xL
Bcl-2
Apaf-1
caspase-3
actin
B
Cyn
0 μg/ml
0.1 μg/ml
0.2 μg/ml
0.4 μg/ml
7-aminoactinomycin D
Multi-caspase
HCT116
HCT116-OxR
(1.10±0.10)
(2.30±0.48)
(5.25±0.52)
(21.67±1.07)
(10.48±0.55)
(22.48±0.81)
(17.10±1.26)
(27.68±1.55)
(1.53±0.45)
(2.88±0.26)
(8.33±0.75)
(10.87±0.25)
(10.12±0.84)
(15.85±1.72)
(15.77±0.30)
(24.07±1.05)
Live
***
C
HCT116
HCT116-OxR
Total caspase+ cells (%)
Cyn (μg/ml) 0 0.1 0.2 0.4
D
HCT116
HCT116-OxR
Cell viability (% of control)
Cyn (μg/ml) - - - 0.4 0.4
Z-VAD-FMK (μM) - - 4 - 4
Ox (μM) - 2 - - -

Figure 5. Activation of caspases in CRC cells. CRC cells treated with cynaropicrin at 0, 0.1, 0.2, or 0.4 μg/mL for 48 h. A. Western blot analysis of Bid, Bax, Bcl-xL, Bcl-2, Apaf-1, and caspase-3. Actin was used as the loading control. B. Flow cytometry analysis using the Muse™ Multi-Caspase Kit. C. Proportions of caspase-positive cells. D. CRC cells were pretreated with Z-VAD-FMK (4 μM) for 3 h and then treated with or without cynaropicrin for 48 h. The histogram shows cell viabilities determined by MTT assay. Data are shown as the mean ± standard deviation, (n = 4). $^{**}P < 0.01$ and $^{***}P < 0.001$ versus untreated controls. $^{###}P < 0.001$ versus cynaropicrin-treated cells.

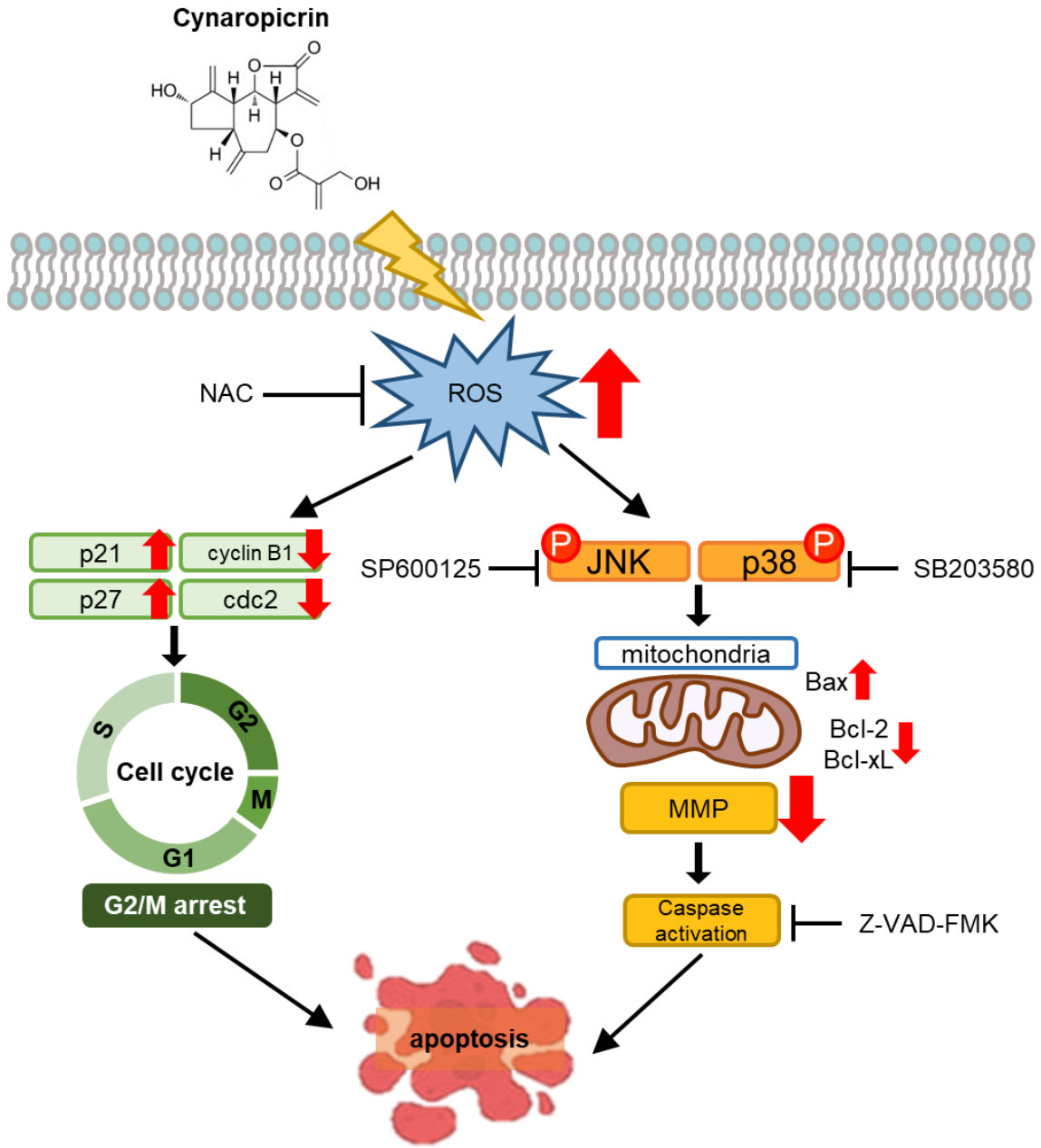

Figure 6. Schematic diagram illustrating the mechanisms by which cynaropicrin induces apoptosis in CRC cells, viz., by generating excessive ROS, activating JNK and p38 MAPK signaling, and inducing cell cycle arrest in the G2/M phase.

tion was upstream of the phosphorylations of JNK and p38 MAPK.

Cell cycle progress is another therapeutic target in cancers [35]. We observed that cynaro-

picrin induced an increase in the percentage of cells in the sub-G1 phase (**Figure 4A**, **4B**), which is an indication of apoptosis [36]. Also, cell cycle distributions indicated that cells in the G2/M phase accumulated, whereas the proportion of cells in the S phase diminished, indicating cell cycle arrest at the G2/M phase (**Figure 4C**). Moreover, cynaropicrin-induced decreases in the levels of cyclin B1 and cdc2, key regulators of G2/M transition and increases in the levels of the CDK inhibitors p21 and p27 [37] indicate that cynaropicrin induced cell cycle arrest at the G2/M phase by modulating cell cycle regulators (**Figure 4D**, **4E**).

In addition to the activations of JNK and p38 MAPK, ROS play a crucial role in regulating the levels of Bcl-2 family proteins [38], and these proteins regulate mitochondrial membrane permeability, thereby mediating the intrinsic apoptotic pathway [39]. Indeed, Western blot analysis showed that the balance between pro- and anti-apoptotic Bcl-2 family proteins had shifted in favor of mitochondrial membrane permeabilization, which was accompanied by the activation of the intrinsic apoptotic pathway, as evidenced by increases in the level of Apaf-1 and cleaved caspase-3 (**Figure 5A**). Encouraged by the increase in the level of cleaved caspase-3, we used a multi-caspase assay kit to assess the activation of caspases (**Figure 5B**, **5C**), as caspases are key molecules in the apoptotic process [40]. As was expected, caspase activation was observed in cynaropicrin-treated cells, thus supporting that the activation of caspases is involved in cynaropicrin-induced apoptosis. This notion was confirmed by pretreating the caspase inhibitor Z-VAD-FMK, which prevented cynaropicrin-induced apoptosis (**Figure 5D**).

In conclusion, the study demonstrates that cynaropicrin inhibits the growth of CRC HCT116 cells, regardless of Ox-resistance. Cynaropicrin elevated ROS levels, activated JNK and p38 MAPK, induced cell cycle arrest, and caused apoptosis. Further studies are warranted to evaluate the therapeutic potential of cynaropicrin in CRC (**Figure 6**).

Acknowledgements

This work was supported by the National Research Foundation of Korea (NRF) grants funded by the Korea government (MSIT) (RS-2022-NR070862 and RS-2024-00336900).

Disclosure of conflict of interest

None.

Address correspondence to: Jin Woo Park and Jung-Hyun Shim, Department of Biomedicine, Health and Life Convergence Sciences, BK21 Four, College of Pharmacy, Mokpo National University, Muan 58554, Republic of Korea. Tel: +82-61-450-2704; E-mail: jwpark@mokpo.ac.kr (JWP); Tel: +82-61-450-2684; E-mail: s1004jh@gmail.com (JHS)

References

[1] Sung H, Ferlay J, Siegel RL, Laversanne M, Soerjomataram I, Jemal A and Bray F. Global cancer statistics 2020: GLOBOCAN estimates of incidence and mortality worldwide for 36 cancers in 185 countries. CA Cancer J Clin 2021; 71: 209-249.

[2] Siegel RL, Wagle NS, Cercek A, Smith RA and Jemal A. Colorectal cancer statistics, 2023. CA Cancer J Clin 2023; 73: 233-254.

[3] Akimoto N, Ugai T, Zhong R, Hamada T, Fujiyoshi K, Giannakis M, Wu K, Cao Y, Ng K and Ogino S. Rising incidence of early-onset colorectal cancer - a call to action. Nat Rev Clin Oncol 2021; 18: 230-243.

[4] Singh U, Kokkanti RR and Patnaik S. Beyond chemotherapy: exploring 5-FU resistance and stemness in colorectal cancer. Eur J Pharmacol 2025; 991: 177294.

[5] Adebayo AS, Agbaje K, Adesina SK and Olajubutu O. Colorectal cancer: disease process, current treatment options, and future perspectives. Pharmaceutics 2023; 15: 2620.

[6] Kumar A, Gautam V, Sandhu A, Rawat K, Sharma A and Saha L. Current and emerging therapeutic approaches for colorectal cancer: a comprehensive review. World J Gastrointest Surg 2023; 15: 495-519.

[7] Bozzuto G, Calcabrini A, Colone M, Condello M, Dupuis ML, Pellegrini E and Stringaro A. Phytocompounds and nanoformulations for anticancer therapy: a review. Molecules 2024; 29: 3784.

[8] Lee SO, Joo SH, Kwak AW, Lee MH, Seo JH, Cho SS, Yoon G, Chae JI and Shim JH. Podophyllotoxin induces ROS-mediated apoptosis and cell cycle arrest in human colorectal cancer cells via p38 MAPK signaling. Biomol Ther (Seoul) 2021; 29: 658-666.

[9] Cech NB and Oberlies NH. From plant to cancer drug: lessons learned from the discovery of taxol. Nat Prod Rep 2023; 40: 1153-1157.

[10] Dhyani P, Quispe C, Sharma E, Bahukhandi A, Sati P, Attri DC, Szopa A, Sharifi-Rad J, Docea AO, Mardare I, Calina D and Cho WC. Anticancer

potential of alkaloids: a key emphasis to colchicine, vinblastine, vincristine, vindesine, vinorelbine and vincamine. Cancer Cell Int 2022; 22: 206.
[11] Chaudhry GE, Md Akim A, Sung YY and Sifzizul TMT. Cancer and apoptosis: the apoptotic activity of plant and marine natural products and their potential as targeted cancer therapeutics. Front Pharmacol 2022; 13: 842376.
[12] Wei Q and Zhang YH. Flavonoids with anti-angiogenesis function in cancer. Molecules 2024; 29: 1570.
[13] Yao P, Liang S, Liu Z and Xu C. A review of natural products targeting tumor immune microenvironments for the treatment of lung cancer. Front Immunol 2024; 15: 1343316.
[14] Miyata Y, Mukae Y, Harada J, Matsuda T, Mitsunari K, Matsuo T, Ohba K and Sakai H. Pathological and pharmacological roles of mitochondrial reactive oxygen species in malignant neoplasms: therapies involving chemical compounds, natural products, and photosensitizers. Molecules 2020; 25: 5252.
[15] Schumacker PT. Reactive oxygen species in cancer: a dance with the devil. Cancer Cell 2015; 27: 156-157.
[16] Sreevalsan S and Safe S. Reactive oxygen species and colorectal cancer. Curr Colorectal Cancer Rep 2013; 9: 350-357.
[17] Sullivan LB and Chandel NS. Mitochondrial reactive oxygen species and cancer. Cancer Metab 2014; 2: 17.
[18] Temkin V and Karin M. From death receptor to reactive oxygen species and c-Jun N-terminal protein kinase: the receptor-interacting protein 1 odyssey. Immunol Rev 2007; 220: 8-21.
[19] Xiong S, Chng WJ and Zhou J. Crosstalk between endoplasmic reticulum stress and oxidative stress: a dynamic duo in multiple myeloma. Cell Mol Life Sci 2021; 78: 3883-3906.
[20] Simon HU, Haj-Yehia A and Levi-Schaffer F. Role of reactive oxygen species (ROS) in apoptosis induction. Apoptosis 2000; 5: 415-418.
[21] Shimoda H, Ninomiya K, Nishida N, Yoshino T, Morikawa T, Matsuda H and Yoshikawa M. Anti-hyperlipidemic sesquiterpenes and new sesquiterpene glycosides from the leaves of artichoke (Cynara scolymus L.): structure requirement and mode of action. Bioorg Med Chem Lett 2003; 13: 223-228.
[22] De Cicco P, Busa R, Ercolano G, Formisano C, Allegra M, Taglialatela-Scafati O and Ianaro A. Inhibitory effects of cynaropicrin on human melanoma progression by targeting MAPK, NF-kappaB, and Nrf-2 signaling pathways in vitro. Phytother Res 2021; 35: 1432-1442.
[23] Cho JY, Kim AR, Jung JH, Chun T, Rhee MH and Yoo ES. Cytotoxic and pro-apoptotic activities of cynaropicrin, a sesquiterpene lactone, on the viability of leukocyte cancer cell lines. Eur J Pharmacol 2004; 492: 85-94.
[24] Lepore SM, Maggisano V, Lombardo GE, Maiuolo J, Mollace V, Bulotta S, Russo D and Celano M. Antiproliferative effects of cynaropicrin on anaplastic thyroid cancer cells. Endocr Metab Immune Disord Drug Targets 2019; 19: 59-66.
[25] Bose D, Zimmerman LJ, Pierobon M, Petricoin E, Tozzi F, Parikh A, Fan F, Dallas N, Xia L, Gaur P, Samuel S, Liebler DC and Ellis LM. Chemoresistant colorectal cancer cells and cancer stem cells mediate growth and survival of bystander cells. Br J Cancer 2011; 105: 1759-1767.
[26] Grana X and Reddy EP. Cell cycle control in mammalian cells: role of cyclins, cyclin dependent kinases (CDKs), growth suppressor genes and cyclin-dependent kinase inhibitors (CKIs). Oncogene 1995; 11: 211-219.
[27] Comella P, Casaretti R, Sandomenico C, Avallone A and Franco L. Role of oxaliplatin in the treatment of colorectal cancer. Ther Clin Risk Manag 2009; 5: 229-238.
[28] Marzi L, Combes E, Vie N, Ayrolles-Torro A, Tosi D, Desigaud D, Perez-Gracia E, Larbouret C, Montagut C, Iglesias M, Jarlier M, Denis V, Linares LK, Lam EW, Martineau P, Del Rio M and Gongora C. FOXO3a and the MAPK p38 are activated by cetuximab to induce cell death and inhibit cell proliferation and their expression predicts cetuximab efficacy in colorectal cancer. Br J Cancer 2016; 115: 1223-1233.
[29] Li F, Huang T, Tang Y, Li Q, Wang J, Cheng X, Zhang W, Zhang B, Zhou C and Tu S. Utidelone inhibits growth of colorectal cancer cells through ROS/JNK signaling pathway. Cell Death Dis 2021; 12: 338.
[30] Kwak AW, Lee MJ, Lee MH, Yoon G, Cho SS, Chae JI and Shim JH. The 3-deoxysappanchalcone induces ROS-mediated apoptosis and cell cycle arrest via JNK/p38 MAPKs signaling pathway in human esophageal cancer cells. Phytomedicine 2021; 86: 153564.
[31] Chun KS and Joo SH. Modulation of reactive oxygen species to overcome 5-fluorouracil resistance. Biomol Ther (Seoul) 2022; 30: 479-489.
[32] Weng MS, Chang JH, Hung WY, Yang YC and Chien MH. The interplay of reactive oxygen species and the epidermal growth factor receptor in tumor progression and drug resistance. J Exp Clin Cancer Res 2018; 37: 61.
[33] Prasad S, Gupta SC and Tyagi AK. Reactive oxygen species (ROS) and cancer: role of antioxidative nutraceuticals. Cancer Lett 2017; 387: 95-105.
[34] Moloney JN and Cotter TG. ROS signalling in the biology of cancer. Semin Cell Dev Biol 2018; 80: 50-64.

[35] Otto T and Sicinski P. Cell cycle proteins as promising targets in cancer therapy. Nat Rev Cancer 2017; 17: 93-115.
[36] Darzynkiewicz Z, Bruno S, Del Bino G, Gorczyca W, Hotz MA, Lassota P and Traganos F. Features of apoptotic cells measured by flow cytometry. Cytometry 1992; 13: 795-808.
[37] Malumbres M and Barbacid M. Cell cycle, CDKs and cancer: a changing paradigm. Nat Rev Cancer 2009; 9: 153-166.
[38] Hildeman DA, Mitchell T, Aronow B, Wojciechowski S, Kappler J and Marrack P. Control of Bcl-2 expression by reactive oxygen species. Proc Natl Acad Sci U S A 2003; 100: 15035-15040.
[39] Kluck RM, Bossy-Wetzel E, Green DR and Newmeyer DD. The release of cytochrome C from mitochondria: a primary site for Bcl-2 regulation of apoptosis. Science 1997; 275: 1132-1136.
[40] Van Opdenbosch N and Lamkanfi M. Caspases in cell death, inflammation, and disease. Immunity 2019; 50: 1352-1364.